Low temperature air-annealing of Cu(InGa)Se$_2$ single crystals

M.V. Yakushev [a,*], A. Jack [a], I. Pettigrew [a], Y. Feofanov [a], A.V. Mudryi [b], J. Krustok [c]

[a] Department of Physics, John Anderson Building, 107 Rottenrow, Strathclyde University, G4 0NG Glasgow, UK
[b] Institute of Solid State and Semiconductor Physics, National Academy of Science, 220072 Minsk, Belarus
[c] Tallinn Technical University, Ehitajate tee 5, Tallinn 19086, Estonia

Abstract

CuInSe$_2$ and CuIn$_{0.95}$Ga$_{0.05}$Se$_2$ single crystals, grown by vertical Bridgman, were annealed in air at temperatures from 100 to 160 °C. Both CuInSe$_2$ and CuIn$_{0.95}$Ga$_{0.05}$Se$_2$ samples were studied using photoluminescence (PL). The CuInSe$_2$ samples were also studied using Rutherford Backscattering Channeling (RBS/C) and nuclear reaction analysis (NRA). Before annealing the samples showed low dechanneling parameters suggesting high quality lattice structure. The PL spectra of both CuInSe$_2$ and CuIn$_{0.95}$Ga$_{0.05}$Se$_2$ revealed bands associated with band-tail recombination mechanism. Annealing at 120 °C and higher temperatures considerably modified the RBS/C and PL spectra. NRA indicated a gradual increase in the oxygen content. PL analysis suggested that annealing increases both the mean-square amplitude of potential fluctuations and the level of compensation. Changes in the RBS/C spectra demonstrated that annealing at up to 160 °C does not result in the growth of In$_2$O$_3$ surface layer but modifies primarily the Se- and Cu-related RBS/C yield. These modifications are consistent with an increase in the concentration of defect complexes.
© 2006 Elsevier B.V. All rights reserved.

Keywords: CuInGaSe$_2$; Oxygen; Photoluminescence

1. Introduction

The ternary chalcopyrite CuInSe$_2$ and its alloy Cu(InGa)Se$_2$ draw a great attention because of their successful application in the solar cell absorber layer. Cu(InGa)Se$_2$/CdS heterojunction solar cells achieved efficiency close to 20% [1]. Annealing of Cu(InGa)Se$_2$ absorbers prior CdS deposition at about 200 °C in air leads to considerable improvements in the performance of the solar cells [2]. This was attributed to the passivation of the positively charged grain-boundary surface donors V_{Se} (selenium vacancies) by oxygen [3]. An air-annealing step is used for most of the present day CuInSe$_2$-based photovoltaic (PV) devices. Recent studies on modification of the electrical properties of bare CuInSe$_2$ and CuInGaSe$_2$, caused by air-annealing at temperatures of 200 °C and above, demonstrated considerable improvements in the Hall parameters. PL spectra taken before and after the treatment indicated that a significant fraction of defects had been passivated [4]. A broad band PL spectrum, attributed to band-tail recombination changed

following oxygen treatment for a donor–acceptor pair (DAP) recombination and an excitonic feature. However, along with the improved opto-electrical properties of the material, a parasitic In$_2$O$_3$ layer was found on the surface [5]. The formation of this layer is followed by the appearance of Cu$_x$Se at the interface with CuInSe$_2$. A study of air-annealed heterostructures of CdS/Cu(InGa)Se$_2$ [6] demonstrated a much greater complexity of physical processes related to oxygen than was observed earlier. It was found that oxygen can reduce the device performance. The presence of oxygen induces the liberation of Cu$^+$, which migrates into the bulk under the influence of the built-in electric field of the hetero-junction, and enhances undesirable recombination in the space-charge region. Cu$^+$ is already mobile at 80 °C, and at 200 °C it is easily driven into the bulk [7]. Thus, despite some advantages of air-annealing at temperatures of 200 °C and higher, such treatment introduces some detrimental features. In contrast annealing at temperatures below 200 °C has been studied very little and may have a potential of reducing the detrimental effects of oxygen without losing the benefits.

In the present report photoluminescence (PL), Rutherford Backscattering Spectrometry in channelling mode (RBS/C) along with Nuclear Reaction Analysis (NRA) have been used

* Corresponding author. Tel.: +44 141 548 3374; fax: +44 141 552 2891.
 E-mail address: michael.yakushev@strath.ac.uk (M.V. Yakushev).

to study the physical processes taking place in the near surface layer of $CuInSe_2$ and $Cu(InGa)Se_2$ due to annealing in air at temperatures from 100 to 160 °C.

2. Experimental details

$CuInSe_2$ and $CuIn_{0.95}Ga_{0.05}Se_2$ single crystals have been cut from the ingot, grown using vertical Bridgman technique, perpendicular to the <221> axis. The samples were mechanically polished through different grades of diamond paste and finally in a vibrator bath with 0.05 μm Al_2O_3 powder. In order to remove the mechanical damage the samples were etched in 0.1% Br in methanol solution for 1 min and then annealed for 0.5 h in vacuum to remove the layer of Se left on the surface due to Br etching as described in detail in [8]. The RBS/C measurements were carried out using 2 meV He^+ ions in the normal incident beam geometry and with 168° backscattering angle. The energy resolution of the analysis was about 25 keV. The orientation of the crystal surface was within 5° from the (112) plane. The homogeneity of the lattice was established by taking the aligned spectra at various points across the surface prior to implantation. A reference normalised minimum-yield $\chi_{min} = Y_{amin} / Y_r$, characterising the dechannelling rate, where Y_{amin} is the minimum backscattering yield in the aligned spectra and Y_r is the backscattering yield in the random spectrum measured at the same energy. For the examined <221> axis $\chi_{min} = 6.2 \pm 0.2\%$ at any point across the surface suggesting that the samples are high structural quality single crystals. Nuclear reaction analysis (NRA) $O^{16}(d,a)N^{17}$ with energy of deuterons 960 keV was used to measure the amount of oxygen in the near surface region. Both RBS/C and NRA measurements were curried out at room temperature. Deuterons of this energy go to the depth of several micrometers making possible to detect all atoms of oxygen penetrated into the crystal during the air annealing at conditions used in the experiment. The samples were annealed for 2 h in air at temperatures 100, 120, 140 and 160 °C.

For PL measurements the samples were cooled, using a closed-cycle He cryostat, to temperatures from 15 to 300 K and excited with the 514 nm line of an Ar laser with maximum output power of about 40 mW. The PL signal was recorded using standard lock-in technique, computer-controlled 1 m grating monochromator and a liquid nitrogen cooled Ge detector.

3. Results and discussion

An asymmetric bands P1, at about 0.93 eV, can be seen in the PL spectra (shown in Fig. 1a) of the non-annealed n-type $CuInSe_2$ sample at 20 K. Several sharper features on the low energy slope of the peak are attributed to water absorption. These absorption features appear in the PL spectra taken during wet weather periods in Glasgow. The temperature and excitation intensity dependencies, shown in Fig. 1, were measured to identify the origin of the band. An increase in the excitation intensity from 1 to 30 mW resulted in a significant blue shift of the band, shown in Fig. 1a,b. This band was shifting at a rate of $j = 12.6$ meV per decade. Such significant j-shift suggests that this band cannot be attributed to a donor–acceptor pair recombination but is associated with band-tails. In highly doped semiconductors spatial potential fluctuations, due to a large number of randomly distributed charged defects, generate band-tails. If the defect concentration is so high that the average distance between two defects becomes smaller than their Bohr radii then the wave-functions of these defects overlap. Their energy levels are spread forming bands and the material becomes heavily doped [9]. The band gap E_g in such semiconductor is smaller than that of the low doped one E_{g0} as shown in Fig. 1e. The condition of high doping for donors and acceptors can be different if the effective
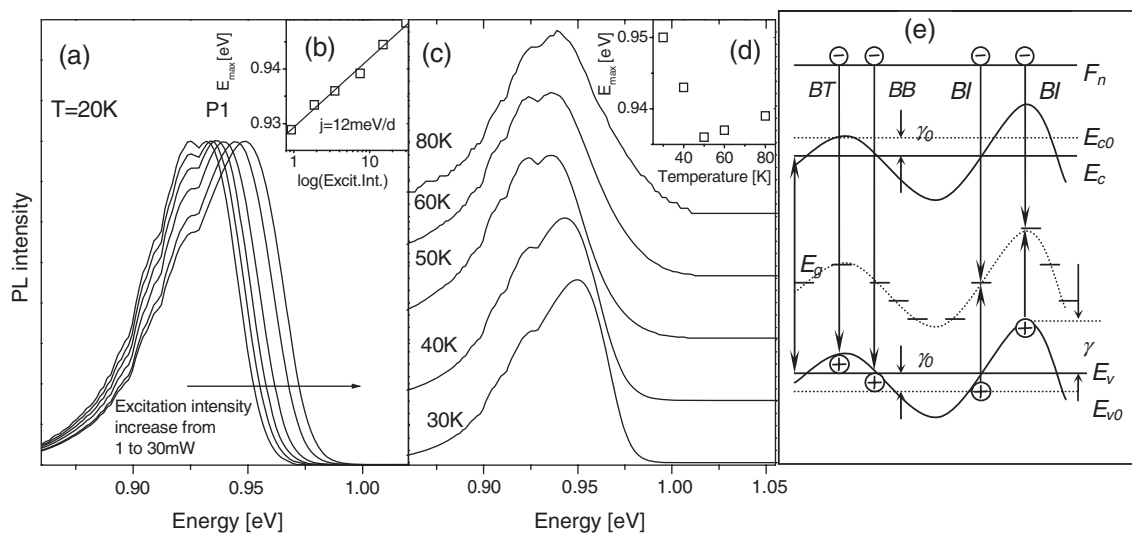

Fig. 1. Excitation intensity dependence of the PL spectra in non-annealed $CuInSe_2$ (a); shift of the maximum of the P1 band at logarithmic increase in the excitation intensity in non-annealed $CuInSe_2$ (b); temperature dependence of the PL spectra in non-annealed $CuInSe_2$ (c); shift of the maximum of the P1 band with temperature in non-annealed $CuInSe_2$ (d); energy diagram of the proposed radiative recombination mechanisms in $CuInSe_2$ (e).

masses of the electron m_e^* and hole m_h^* differ considerably. In CuInSe$_2$ holes are significantly heavier than electrons $m_h^*=0.73m_e$ [10] and $m_e^*=0.09m_e$ [11]. This material contains both donors and acceptors revealing n-type conductivity if the concentration of donors is higher and p-type if it is lower. The high doping conditions can easier be achieved for donors. At high concentration of donors the conduction band E_c becomes highly filled. The distribution of electrons can be described by introducing a Fermi-level for electrons F_n. Their kinetic energy $F_n - E_c$ considerably exceeds the potential energy of their coupling. Holes are heavy and can be considered as classical particles. At low temperatures they are localised at deep hydrogenic states of the valence band-tail acting like acceptor levels. A good approximation of the density of states in such band-tails is $\rho_v(\varepsilon) \sim \exp(-\varepsilon/\gamma_0)$ [9], where γ_0 is the mean-square depth of the potential energy-fluctuations, ε is the energy of a hole measured above the valence band $\varepsilon = E_h - E_v > 0$. If the condition of high doping is not realised for acceptors with ionisation energy $I_a(\gamma_0 < I_a)$ their wave-functions do not overlap. These acceptor levels do not form an impurity band remaining outside the valence band-tail, as shown in Fig. 1e. The shape of the PL peak, associated with these levels, is affected by the spatial potential fluctuations and γ_0. At low temperatures the radiative recombination can arise from two different channels, shown in Fig. 1e, a free electron and a hole localised in the valence band-tail (BT), and a band-impurity (BI) recombination involving the acceptor-state. At higher temperatures (above 100 K) the free electron-free hole (BB) band can appear.

The high value of the j-shift, observed for the band in the non-annealed sample, suggests that this band is associated with the BT recombination. Several other signs also indicate this assignment. The specific shape of the band, broad and asymmetrical, suggests the BT nature of the band. The experimental spectra were fitted with the empirical asymmetric double sigmoidal function $I(h\nu)=A(1/(1+\exp[-(h\nu-E_1)/W_1]))*(1-1/(1+\exp[-(h\nu-E_1)/W_2]))$ where A, E_1, E_2, W_1 and W_2 are the fitting parameters (E_1, W_1 and E_2, W_2 represent the shape of the low- and high-energy sides of the PL bands, respectively) suggested in [12] for BT-type bands. This fitting considerably increases the accuracy of the analysis. An example of such fitting is shown in Fig. 2a. Changes in the PL spectra in the non-annealed sample are shown in Fig. 1c. The temperature dependence of the P1 peak maximum spectral position (E_{max}), shown in Fig. 1d, exposes a minimum T_{min}, which is a characteristic parameter in the theory of heavily doped semiconductors [9]. The slope of this curve at temperatures below T_{min} and the value of T_{min} were used to derive the mean square amplitude of the potential fluctuation γ_0 of the sample before oxidation $\gamma_0=19.4$ meV [13]. The low-energy side of BT-band is defined by the density of state in the valence band-tails $\rho_v(\varepsilon)$. The shape of this side does not depend on temperature or excitation intensity. The high-energy side has a more complex nature. At low temperatures ($kT < \gamma_0$) the high-energy slope does not depend on temperature but at higher temperatures ($kT > \gamma_0$) it decreases linearly with temperature making the BT-band more symmetrical.

The PL spectra in CuIn$_{0.95}$Ga$_{0.05}$Se$_2$ before oxidation revealed a higher energy broad and asymmetrical band P1 and a deeper band P2 shown in Fig. 2b. Analysis of the temperature and excitation intensity dependencies also suggested that the P1 peak is associated with BT transition. The j-shift of the P1 peak was 10.8 meV/decade. The mean square depth of potential fluctuations before oxidation was found to be $\gamma_0=15$ meV. The origin of the P2 band was also identified from the excitation and temperature dependencies of the PL spectra.
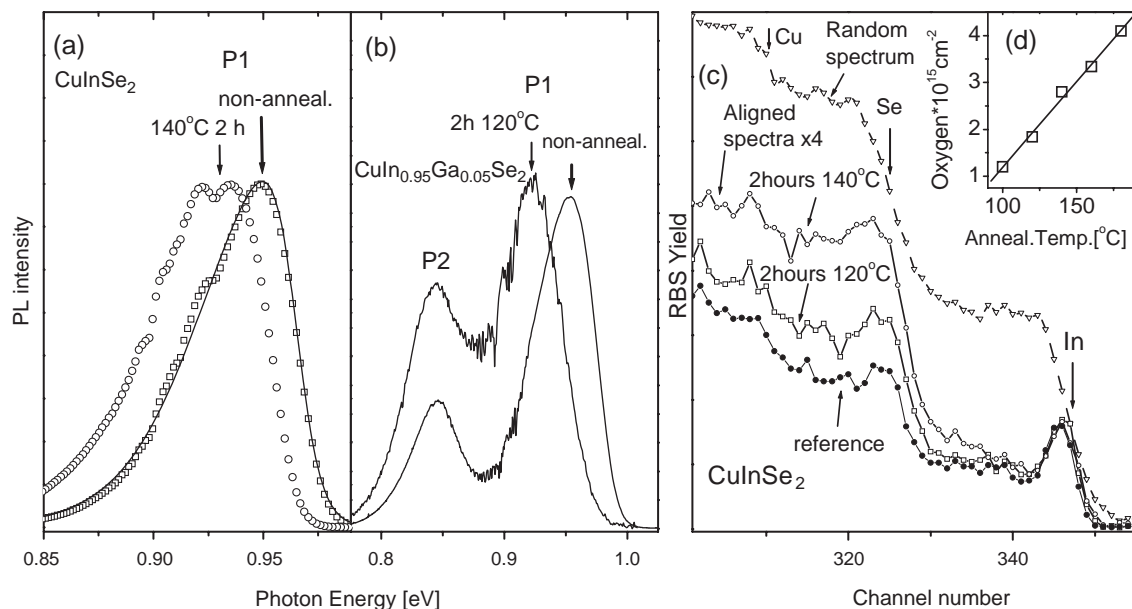

Fig. 2. The PL spectra in CuInSe$_2$ before (□) and after (○) 2 h annealing at 140 °C in air, the dashed lines show the double-Lorentzian curve fitted into the experimental spectrum (a); the PL spectra in CuIn$_{0.95}$Ga$_{0.05}$Se$_2$ before and after 1 h annealing at 120 °C in air (b); aligned and random RBS spectra before and after 2 h at 120 and 140 °C annealing in air (c); changes in the content of oxygen after annealing in air for 2 h at different temperatures measured by NRA (d).

Excitation intensity increase resulted in a 1–2 meV/decade *j*-shift of the P2 band. Also, the spectral position of the P2 peak was slightly shifting towards low energy at temperature increasing up to about 55 K. At higher temperatures the peak shifted towards high energy. Taking into account these results it is reasonable to associate the P2 band with band-to-deep-level optical transition (BI). The deep level is more likely to be a deep acceptor. A diagram of this transition is shown in Fig. 1e. In low-doped semiconductors the maximum of BI band has a *j*-shift of about 1–2 meV/decade and depends on temperature as $E_{max} = E_{g0} - I_a + 0.5kT$, where E_{g0} is the band-gap at low levels of doping. In highly doped semiconductors the BI-band maximum follows a more complex dependence on temperature [14] forming a minimum as observed in the present experiment. The shape of the BI band is also asymmetrical. The low-energy slope is formed by the recombination of the holes localised at the valence band-tails, with γ_0 as a parameter. The high-energy slope is affected by temperature and at low temperature it is steeper than the low energy slope. The acceptor activation energy I_a could not be derived from an Arrhenius plot because the position of the level is spread by the potential fluctuations and in the Ln(I) versus $1000/T$ dependence no straight lines can be found.

Annealing in air at 100 °C for 2 h did not change the shape of the PL spectra. After annealing at 120 °C and higher, the intensity of the PL emission becomes considerably lower. The spectral position of the band shifts towards lower energies becoming broader. These changes can be seen in Fig. 2a for CuInSe$_2$, where PL spectra before and after 140 °C annealing for 2 h are shown, and in Fig. 2b for CuIn$_{0.95}$Ga$_{0.05}$Se$_2$, before and after 120 °C annealing for 1 h. Analysis of the temperature dependence of the band P1 in CuInSe$_2$ indicates an increase in the *j*-shift, which after 140 °C 2 h annealing becomes 22.5 meV/decade. In CuIn$_{0.95}$Ga$_{0.05}$Se$_2$ the *j*-shift of the P1 peak also increased up to 21.4 meV/decade after 1 h 120 °C oxidation. Analysis of the temperature dependencies of the peak P1 in both compounds suggests that the mean depth of the potential fluctuations also increased due to this annealing becoming $\gamma_0 = 21.7$ meV for CuInSe$_2$ and $\gamma_0 = 21$ meV for CuIn$_{0.95}$Ga$_{0.05}$Se$_2$. Further increase in both the temperature and the time of annealing reduced further the intensity of the PL emission suggesting an increase in the concentration of non-radiative traps. Partial substitution of In by Ga made the material more susceptible to oxidation because strong changes were observed in the CuIn$_{0.95}$Ga$_{0.05}$Se$_2$ PL spectra at lower temperatures and shorter times of annealing than in CuInSe$_2$.

The lattice structure of the CuInSe$_2$ samples was examined using RBS/C and NRA techniques to understand the nature of the observed changes in the PL spectra. The random spectra did not reveal any signs of stoichiometry deviation after air-annealing up to 160 °C. Changes in the aligned spectra, shown in Fig. 2c, become considerable after annealing at temperature from 120 °C. The surface peak in the indium yield remains the same suggesting that the In$_2$O$_3$ layer on the surface did not grow. Beyond the surface peak the slope of the indium-related yield in the RBS aligned spectra did not increase after 120 °C

annealing and increased very little after 140 °C one suggesting that no indium moved into interstitial positions. Indium remains on the regular lattice sites. The slight increase in the slope can be associated with the dechannelling due to an increase in the dispersion of the channelling ion beam. No single-scattering from In can be seen nether after 120 nor after 140 °C. These changes could be explained by the presence of Cu, Se or/and O in interstitial positions of the lattice. The selenium related yield demonstrates a very different dechannelling. A considerable increase in the Se-related yield can be clearly seen. These changes are associated with interstitially located Se atoms. It is more difficult to make a confident conclusion about the copper-related yield because it is located on the top of the In and Se ones, and is quite low in magnitude due to the low atomic number of this element. However, an increase in the Cu-related yield also seems to be present. NRA measured amount of oxygen, shown in Fig. 2d, indicates a gradual increase in the oxygen content with the temperature of annealing. Because this oxygen does not incorporate into the In$_2$O$_3$ layer it must be diffusing into the bulk of the sample. A possibility of the presence of oxygen on selenium site O$_{Se}$ on the surface has been discussed earlier [3,15]. Such oxygen was observed directly using scanning probe microscopy [16]. Oxygen diffusing into the crystal from air may also take selenium vacancies in the bulk. Although the compound CuInO$_2$ cannot exist [15] a fraction of selenium vacancies can be filled with oxygen. This would stabilise the lattice and explain the low dechannelling observed for the In sublattice. The high dechannelling rate associated with the Se and Cu sublattices can be explained by the presence of interstitial Cu$_i$, Se$_i$ and O$_i$ or defect-complexes including these atomic species. A mechanism of oxygen-induced copper release has been proposed earlier [6]. Interstitial selenium is expected to diffuse towards the surface. This is supported by the increase in the surface peak in the Se related yield, which can be seen in Fig. 2c. Interstitial copper is known to migrate into the bulk creating a gradient of copper at the surface. An increase in the annealing temperature raises the number of copper and selenium atoms released from their lattice sites into interstitial positions. The formation of Cu$_x$Se can also be expected [6]. The appearance of p-type Cu$_x$Se in the n-type material should increase the level of compensation. This model is supported by the PL data indicating an increase in the *j*-shift after the annealing. The observed rise in the mean-square amplitude of potential fluctuation can be explained by the copper depletion increasing the In/Cu ratio. Low temperature air-annealing offers an interesting method to deliver oxygen into the bulk of Cu(InGa)Se$_2$ without increasing the width of In$_2$O$_3$ layer on the surface. However, this treatment increases the amplitude of potential fluctuation and the level of compensation.

4. Conclusion

Low temperature annealing of Cu(InGa)Se$_2$ single crystals in air does not promote the growth of the In$_2$O$_3$ layer but results in a diffusion of oxygen into the near-surface layer. Such

annealing results in the formation of defect-complexes containing selenium, copper and oxygen atoms raising the mean-square amplitude of potential fluctuations and the compensation level of the material.

References

[1] K. Ramanathan, M. Contreras, C. Perkins, S. Asher, F. Hasoon, J. Keane, D. Young, M. Romero, W. Metzger, R. Noufi, J. Ward, A. Duda, in: Progress in Photovoltaics: Research and Applications, vol. 11, 2003, p. 225.

[2] R.W. Birkmire, L.C. DiNetta, P.G. Lasswell, J.D. Meakin, J.E. Phillips, Sol. Cells 16 (1986) 419.

[3] D. Cahen, R. Nouffi, Appl. Phys. Lett. 54 (1989) 558.

[4] I. Dirnstorfer, W. Burkhardt, W. Kriegseis, I. Osterreicher, H. Alves, D.M. Hofmann, O. Ka, A. Polity, B.K. Meyer, D. Braunger, Thin Solid Films 361–362 (2000) 400.

[5] G.A. Medvedkin, G.A. Ambrazevichius, A.A. Yakovenko, Surf. Investig.: X-Ray Synchrotron Neutron Tech. 2 (1987) 81.

[6] U. Rau, D. Braunger, R. Herberholz, H.W. Shock, J.F. Guillemoles, L. Kronok, D. Cahen, J. Appl. Phys. 86 (1999) 497.

[7] V. Nadazdy, M. Yakushev, E.D. Djebbar, A.E. Hill, R.D. Tomlinson, J. Appl. Phys. 84 (1998) 4322.

[8] M.V. Yakushev, G. Lippold, A.E. Hill, R.D. Pilkington, R.D. Tomlinson, J. Mater. Sci., Mater. Electron. 7 (1996) 155.

[9] A.P. Levanyuk, V.V. Osipov, Sov. Phys., Usp. 24 (1981) 187.

[10] T. Irie, S. Endo, S. Kimura, Jpn. J. Appl. Phys. 18 (1979) 1303.

[11] H. Weinert, H. Neumann, H. Hobler, G. Kuhn, N.V. Nam, Phys. Status Solidi, B Basic Res. 81 (1977) K59.

[12] J. Krustok, H. Collan, M. Yakushev, K. Hjelt, Phys. Scr., T 79 (1999) 179.

[13] J. Krustok, J. Raudoja, M. Yakushev, R. Pilkington, H. Collan, Phys. Status Solidi, A Appl. Res. 173 (1999) 483.

[14] A. Jagomägi, J. Krustok, J. Raudoja, M. Grossberg, M. Danilson, M. Yakushev, Phys., B Condens. Matter 337 (2003) 369.

[15] G.A. Medvedkin, G.A. Ambrazevichius, A.A. Yakovenko, Surf. Investig.: X-Ray Synchrotron Neutron Tech. 2 (1987) 81.

[16] L. Kazmerski, Jpn. J. Appl. Phys., Suppl. 32-3 (1993) 25.